

NONLINEAR OPTICAL PHENOMENA

PACS numbers: 42.60.Jf; 42.65.An
DOI: 10.1070/QE2015v045n04ABEH015569

Threshold effect under nonlinear limitation of the intensity of high-power light

S.A. Tereshchenko, V.M. Podgaetskii, A.Yu. Gerasimenko, M.S. Savel'ev

Abstract. **A model is proposed to describe the properties of limiters of high-power laser radiation, which takes into account the threshold character of nonlinear interaction of radiation with the working medium of the limiter. The generally accepted non-threshold model is a particular case of the threshold model if the threshold radiation intensity is zero. Experimental *z*-scan data are used to determine the nonlinear optical characteristics of media with carbon nanotubes, polymethine and pyran dyes, zinc selenide, porphyrin-graphene and fullerene-graphene. A threshold effect of nonlinear interaction between laser radiation and some of investigated working media of limiters is revealed. It is shown that the threshold model more adequately describes experimental *z*-scan data.**

Keywords: *limitation of laser radiation intensity, absorption coefficient, nonlinear optical characteristics, pulse shape, nonlinear absorption, z scanning.*

1. Introduction

The necessity of providing a safe level of laser radiation intensity in order to protect organs of vision and sensing elements of optical systems calls for developing limiters of high-power laser intensity and studying their working media. Currently, absorption and interference filters are widely used as protection tools. Drawbacks of neutral absorption light filters are the partial loss of radiation and (in the case of colour light filters) disturbance of colour perception. In interference filters, the effect of attenuation (transmittance) depends on the angle of incidence of light, and protection is provided only in a narrow range of laser wavelengths. In addition, all these filters are linear, i.e., they equally attenuate both high- and low-power laser beams, whereas it is necessary to limit only high-power laser intensity. For the aforementioned reasons, one should search for new ways of limiting high-power laser beam intensity that are based on nonlinear interaction of laser radiation with matter [1–5].

Thus, optical limiters must have low transmittance for high-intensity laser beams and high transmittance for non-hazardous low-intensity radiation. Various nonlinear physical processes may occur in working media of limiters: absorption, refraction and scattering of light; thermal defocusing; etc. [2, 4]. The specific microscopic mechanism of radiation limiting may be either due to one of possible physical processes or to their combination. However, describing properties of limiters based on these specific microscopic mechanisms of intensity limitation, one cannot provide sufficient correspondence between the theoretical and experimental results. Several interaction mechanisms, the degree of influence of which has been studied insufficiently, may act simultaneously in real limiters. In addition, the computation of some microscopic limiting mechanisms is a complex problem, which has not been completely solved to date. The approach in which phenomenologically determined characteristics of the working medium of a limiter are found based on experimental data using the radiation transfer equation appears to be more promising. An advantage of this approach is that it is not necessary to know anything about the specific microscopic mechanisms of intensity limitation and their role. Moreover, it allows one to predict the properties of a limiter with the same working medium but another thickness of the working layer, for another spatial profile in the laser beam cross section, or for another temporal shape of laser pulse. In this study, we used specifically this phenomenological approach. In addition, all results were obtained on the assumption that the limiter working medium is purely absorbing; in other words, there are no any other physical processes that may affect the form of radiation transfer equation.

Many materials that can be used as working media for optical limiters have been experimentally investigated. They include semiconductors [2–4, 6], dyes [1, 3, 7], metals [2–4, 8], porphyrins [9–11], crystals [2, 3] and binary stratified solutions [12]. The advances in nanotechnologies open new ways for developing optical limiters [13]. A study of the optical limitation by nanoparticles with different sizes revealed that the effect of intensity limitation is enhanced with decreasing particle size [14]. Good limiting properties were shown by fullerenes and their derivatives [2, 3], dispersed media based on soot [2], single-wall carbon nanotubes (SWCNTs) and multiwall carbon nanotubes (MWCNTs) [4, 15–17], and hybrid materials based on carbon nanotubes [11, 18–23]. Another allotropic form of carbon, graphene, has not only interesting electronic and mechanical properties [5, 15]. It has been established that dispersed media based on graphene oxide are efficient limiters of light [5, 24, 25]; this limiting property is especially pronounced in dispersed media based on functionilised graphene [5, 10, 25–28]. In addition, the nonlinear characteristics were significantly amplified with a decrease in atmospheric pressure (this decrease facilitates formation and growth of microbubbles and/or microplasma) [29]. Solid composites based on nanotubes or graphene with

S.A. Tereshchenko, V.M. Podgaetskii, A.Yu. Gerasimenko, M.S. Savel'ev National Research University of Electronic Technology (MIET), pl. Shokina 1, Zelenograd, 124498 Moscow, Russia; e-mail: tsa@miee.ru, podgaetsky@yandex.ru, nanobiomedics@gmail.com, sm-s88@mail.ru

Received 28 May 2014; revision received 30 July 2014
Kvantovaya Elektronika **45** (4) 315–320 (2015)
Translated by Yu.P. Sin'kov

organically modified silicon dioxide or polymethylmethacrylate were also investigated [30–32].

On the whole, the properties of a limiter are described by its output characteristic, which is a dependence of the laser pulse energy transmitted through the limiter on the initial pulse energy [33]. The output characteristic describes the efficiency of limiting laser beam intensity.

The output characteristic of a working medium can be experimentally determined using the *z*-scan technique [6], where the total energy of a laser pulse transmitted through a limiter is measured during the sample motion along the beam axis *z* with respect to the of laser beam waist formed by a lens. Generally, *z*-scan data are used to calculate the nonlinear absorption coefficient on the assumption of non-threshold dependence of the absorption coefficient on the laser radiation intensity [33].

In this study, we proposed a threshold model of the dependence of the absorption coefficient on the radiation intensity. Based on this model and using *z*-scan data, we obtained nonlinear characteristics for media with SWCNTs and MWCNTs in dimethylformamide (DMF), tetrahydrofurane (THF) and polymethylmethacrylate (PMMA).

In addition, within the threshold model, we recalculated the nonlinear characteristics of previously investigated materials: ZnSe, porphyrin-graphene (Graphene-TPP), fullerene-graphene (Graphene C_{60}), polyethylene oxide (PEO) with MWCNTs (PEO/MWCNTs) in DMF, polymethine dyes PD-792 and PD-7098, and dicyanomethylene-pyran dyes DCM-627 and DCM-684 [33]. A threshold effect under limitation of radiation intensity was revealed for some working media. The threshold and non-threshold models were compared. It was shown that the threshold model more adequately describes experimental data.

2. Theory

Let the intensity of an initial laser pulse be described by the expression

$$I_0(\rho,\varphi,t) = U_0 A(\rho) B(t), \tag{1}$$

where U_0 is the total pulse energy; ρ and φ are polar coordinates in the laser beam cross section; $A(\rho)$ is the radial pulse profile in the laser beam cross section; and $B(t)$ is the temporal pulse shape. The following normalisation conditions are fulfilled:

$$\int_{-\infty}^{+\infty}\int_0^{2\pi}\int_0^{\infty} I_0(\rho,\varphi,t)\rho\mathrm{d}\rho\mathrm{d}\varphi\mathrm{d}t = U_0,$$

$$\int_0^{\infty} A(\rho)\rho\mathrm{d}\rho = \frac{1}{2\pi},\ \int_{-\infty}^{+\infty} B(t)\,\mathrm{d}t = 1.$$

The transmission of pulsed radiation through a medium with nonlinear absorption can be described in terms of the radiation transfer equation [34]. The nonlinear interaction of laser radiation with matter is generally characterised by absorption coefficient, which depends linearly on the laser pulse intensity *I* (Fig. 1a):

$$\mu(I) = \alpha + \beta I. \tag{2}$$

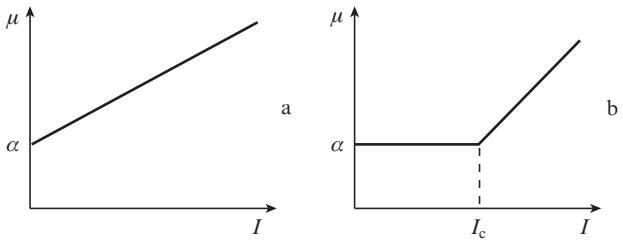

Figure 1. Dependence of the absorption coefficient on radiation intensity for the (a) non-threshold and (b) threshold models.

It is suggested that $\mu(I)$ can be expanded in a Taylor series, which is valid in the entire range from zero to some maximum value I_{max}, and the first two terms of the expansion are retained. Then the nonlinear medium is characterised by two parameters: linear absorption coefficient α (in m^{-1}) and nonlinear absorption coefficient β (in m W^{-1}). Relation (2) will be referred to as the non-threshold model. Note that relation (2) initially suggests the absence of any interaction threshold.

At the same time, it is known that some microscopic mechanisms of interaction between laser radiation and a nonlinear medium have a threshold character [2, 35], i.e., they are switched on at intensities exceeding some threshold value I_c. Therefore, it is expedient to consider a model with an absorption coefficient of threshold type (Fig. 1b):

$$\mu(I) = \begin{cases} \alpha, & I < I_c, \\ \alpha + \beta_c(I - I_c), & I > I_c, \end{cases} \tag{3}$$

where β_c is the nonlinear absorption coefficient in the threshold model. We will refer to relation (3) as the threshold model. Thus, the threshold model is characterised by three parameters: α, β_c and I_c. If $I_c = 0$, then $\beta_c = \beta$ and the threshold model is transformed into the non-threshold one; i.e., the non-threshold approximation is a particular case of the threshold model.

Within the non-threshold model, the solution to the radiation transfer equation for a pulse transmitted through a layer of the limiter working medium of thickness *d* has the form [34]

$$I^{(\mathrm{nt})}(\rho,\varphi,t,d) = \frac{\alpha\exp(-\alpha d) I_0(\rho,\varphi,t)}{\alpha + \beta[1 - \exp(-\alpha d)]I_0(\rho,\varphi,t)}. \tag{4}$$

Within the threshold model, the solution $I^{(\mathrm{th})}(\rho,\varphi,t,d)$ to the radiation transfer equation has a more complex form:

$$I^{(\mathrm{th})}(\rho,\varphi,t,d) = \tag{5}$$

$$\begin{cases} I_0(\rho,\varphi,t)\exp(-\alpha d), & I_0(\rho,\varphi,t) \leqslant I_c, \\ \dfrac{I_c}{\exp(\alpha d)}\left\{\dfrac{\alpha I_0(\rho,\varphi,t)}{[\alpha-\beta_c I_c+\beta_c I_0(\rho,\varphi,t)]I_c}\right\}^{\frac{\alpha}{\alpha-\beta_c I_c}}, & I_c < I_0(\rho,\varphi,t) \leqslant I_1, \\ \dfrac{(\alpha-\beta_c I_c) I_0(\rho,\varphi,t)\exp[-(\alpha-\beta_c I_c)d]}{\alpha-\beta_c I_c+\beta_c I_0(\rho,\varphi,t)\{1-\exp[-(\alpha-\beta_c I_c)d]\}}, & I_0(\rho,\varphi,t) > I_1, \end{cases}$$

where

$$I_1 = \frac{(\alpha - \beta_c I_c) I_c}{\alpha\exp[-(\alpha - \beta_c I_c)d] - \beta_c I_c}.$$

For a Gaussian laser pulse, the profile $A(\rho)$ in the laser beam cross section and the temporal distribution $B(t)$ are Gaussian functions:

$$A(\rho) = \frac{2}{w^2\pi}\exp\left(-\frac{2\rho^2}{w^2}\right), \tag{6}$$

$$B(t) = \frac{1}{\tau\sqrt{\pi}}\exp\left(-\frac{t^2}{\tau^2}\right), \tag{7}$$

where τ is the pulse duration and w is the beam radius.

The total energy U of a pulse transmitted through a limiter, as a function of the total energy of initial pulse, U_0, is an output characteristic of a limiter, which characterises its main properties with respect to intensity limitation:

$$U(U_0) = \int_{-\infty}^{+\infty}\int_0^{2\pi}\int_0^{\infty} I(\rho,\varphi,t,d)\rho\mathrm{d}\rho\mathrm{d}\varphi\mathrm{d}t. \tag{8}$$

In the non-threshold model for a Gaussian pulse, the total energy $U^{(\mathrm{nt})}$ of a pulse transmitted through a limiter is described by the expression [33]

$$U^{(\mathrm{nt})}(U_0) = U_0\exp(-\alpha d)\,\mathrm{ls}\left\{U_0\frac{2\beta[1-\exp(-\alpha d)]}{\alpha\tau w^2\pi^{3/2}}\right\}, \tag{9}$$

where

$$\mathrm{ls}(x) = \frac{2}{x\sqrt{\pi}}\int_0^{+\infty}\ln(1+x\exp(-t^2))\,\mathrm{d}t. \tag{10}$$

In the threshold model for a Gaussian pulse, the total energy of a pulse transmitted through a limiter is described as

$$U^{(\mathrm{th})}(U_0) = U_0\exp(-\alpha d) \tag{11}$$

at $U_0 < \dfrac{I_c w^2\tau\pi^{3/2}}{2}$,

$$U^{(\mathrm{th})}(U_0) = \frac{4}{\sqrt{\pi}}U_0\exp(-\alpha d)\left[\frac{\sqrt{\pi}}{4} - \mathrm{ls}_2(0,1,\sqrt{\ln\gamma})\right.$$

$$\left. + \gamma^{\frac{\xi}{1-\xi}}\mathrm{ls}_2\left(\frac{\xi\gamma}{1-\xi},\frac{1}{1-\xi},\sqrt{\ln\gamma}\right)\right] \tag{12}$$

at $\dfrac{I_c w^2\tau\pi^{3/2}}{2} < U_0 < \dfrac{I_1 w^2\tau\pi^{3/2}}{2}$,

$$U^{(\mathrm{th})}(U_0) = \frac{4}{\sqrt{\pi}}U_0\exp(-\alpha d)\left[\frac{\sqrt{\pi}}{4} - \mathrm{ls}_2(0,1,\sqrt{\ln\gamma})\right.$$

$$+ \gamma^{\frac{\xi}{1-\xi}}\mathrm{ls}_2\left(\frac{\xi\gamma}{1-\xi},\frac{1}{1-\xi},\sqrt{\ln\gamma}\right) - \gamma^{\frac{\xi}{1-\xi}}\mathrm{ls}_2\left(\frac{\xi\gamma}{1-\xi},\frac{1}{1-\xi},\sqrt{\ln\gamma_1}\right)$$

$$\left. + \exp(\alpha\xi d)\,\mathrm{ls}_2\left(\frac{\xi\gamma}{1-\xi}\left(1-\frac{\exp(\alpha\xi d)}{\exp(\alpha d)}\right),1,\sqrt{\ln\gamma_1}\right)\right] \tag{13}$$

at $\dfrac{I_c w^2\tau\pi^{3/2}}{2} < U_0$.

Here $\xi = \dfrac{\beta_c I_c}{\alpha}$; $\gamma = \dfrac{2U_0}{I_c w^2\tau\pi^{3/2}}$; $\gamma_1 = \dfrac{2U_0}{I_1 w^2\tau\pi^{3/2}}$; and

$$\mathrm{ls}_2(a,b,c) = \int_0^c\left\{\left[\frac{b\exp(-r^2)}{1+a\exp(-r^2)}\right]^b r^2\right\}\mathrm{d}r. \tag{14}$$

Thus, the proposed threshold model of nonlinear interaction of laser radiation with matter is characterised by expression (3) for the absorption coefficient and relations (11)–(13), which follow from it.

3. Experimental

As in the case of the non-threshold model, the application of the z-scan technique within the threshold model implies a measurement of the total energy $U^{(\mathrm{e})}(z)$ of a pulse transmitted through a limiter, with a sample being displaced along the z axis with respect to the laser beam waist formed by a lens. The theoretical $U^{(\mathrm{t})}(z)$ values for the threshold model are determined from expressions (11)–(13) in the same way as for the non-threshold model based on expression (9) [33]. The z-scan data are used to find the dependence of normalised transmittance $T^{(\mathrm{e})}$ on displacement z:

$$T^{(\mathrm{e})}(z) = \frac{U^{(\mathrm{e})}(z)}{U_0}\exp(\alpha d). \tag{15}$$

The linear absorption coefficient is determined beforehand for low radiation intensities, at which nonlinear effects are negligible.

Then, using the least-squares method, one can find parameters β_c and I_c for the threshold model by minimising the quadratic functional Φ of deviations of experimental values $T^{(\mathrm{e})}(z)$ of normalised transmittance from the theoretical values $T^{(\mathrm{t})}(z) = [(U^{(\mathrm{t})}(z))/U_0]\exp(\alpha d)$:

$$\Phi = \sum_{n=1}^{N}\left[T^{(\mathrm{e})}(z_n) - T^{(\mathrm{t})}(z_n)\right]^2, \tag{16}$$

where n is the measurement number and N is the number of measurements. The parameter β for the non-threshold model is also calculated for comparison.

The knowledge of the parameters of the limiter working medium, i.e., the values α and β (non-threshold model), or α, β_c and I_c (threshold model), allows one to calculate the output characteristic for not only the sample subjected to z scanning but also for any other thickness of the working medium layer in the limiter and other initial-radiation parameters, with expression (9) for the non-threshold model and expressions (11)–(13) for the threshold model. In addition, one can calculate the theoretical z-scan curve for the obtained parameters and establish the degree of its correspondence to experimental data.

We performed z-scan experiments using a pulsed Nd:YAG laser.The beam waist was formed by a lens with a focal length of 10 cm, and the displacement step of the cell with the working medium was 0.2 cm. The values of the linear absorption coefficient α were determined beforehand in experiments with beams having a low input intensity, at which nonlinear effects are not observed.

We investigated (Table 1) dispersed SWCNT- and MWCNT-containing media with DMF and THF solvents, composites consisting of SWCNTs and MWCNTs in PMMA, solutions of polymethine dyes PD-792 and PD-7098, and solutions of pyran dyes DCM-627 and DCM-684. The following solvents were used for dyes: propylene glycol carbonate (PGC), ethanol and 2-propanol. The concentration and thickness of the limiter working medium were chosen so as to provide the initial transmittance of no less than 50%.

Table 1. Parameters of limiter working media according to *z*-scan data.

No.	Working medium	λ/nm	U_0/μJ	τ/ns	d/cm	α/cm^{-1}	w_0/μm	β/cm GW^{-1}	β_c/cm GW^{-1}	I_c/GW cm^{-2}	References
1	MWCNTs in DMF	532	124	7	0.2	1.93	20	52.0	96	0.026	this study (experiment)
2	MWCNTs in DMFv		182			1.93	20	51.8	104	0.032	
3	MWCNTs in THF		114			2.23	21	98.7	115	0.006	
4	MWCNTs in THF		184			2.23	22	93.1	120	0.008	
5	MWCNTs in PMMA		124		0.54	0.74	21	2.78	2.78	0	
6	SWCNTs in PMMA		120		0.495	0.66	24	2.68	2.68	0	
7	SWCNTs in THF		124		0.2	1.78	21	74.4	125	0.022	
8	SWCNTs in THF		184			1.78	21	63.9	100	0.02	
9	PD-792 in PGC		21	0.35	0.5	0.88	27	5.0	5.5	0.007	
10	PD-7098 in PGC		22			0.57	29	6.9	7.2	0.007	
11	DCM-627 in PGC		22			0.32	33	0.277	0.275	0.004	
12	DCM-684 in PGC		22			0.35	33	0.28	0.28	0	
13	PD-7098 in ethanol		22			0.08	29	6.1	6.0	0.005	
14	PD-7098 in PGC		22			1.17	30	12.4	14.0	0.008	
15	PD-7098 in 2-propanol		22			0.69	27	4.2	4.3	0.007	
16	MWCNTs in DMF	1064	122	7	0.2	1.78	24	63.0	190	0.029	
17	MWCNTs in DMF		188			1.78	24	70.6	190	0.027	
18	MWCNTs in PMMA		122		0.54	0.95	22	0.5	0.5	0	
19	SWCNTs in ПММА		122		0.495	1.03	23	1.59	1.9	0.028	
20	ZnSe		0.1	0.027	0.27	0.27	26	5.9	5.9	0	[6]
21	PEO/MWCNTs in DMF		145	7	1	0.69	32	17	38	0.014	[16]
22	Graphene C_{60}	532	7	5	0.1	2.87	21	132	145	0.0009	[28]
23			15				20	241	245	0.0004	
24			25				21	259	295	0.0007	
25			50				20	442	451	0.0002	
26	Graphene-TPP		7				21	90	90	0	
27			15				21	117	125	0.0006	
28			25				20	144	144	0	
29			50				20	214	216	0.0001	

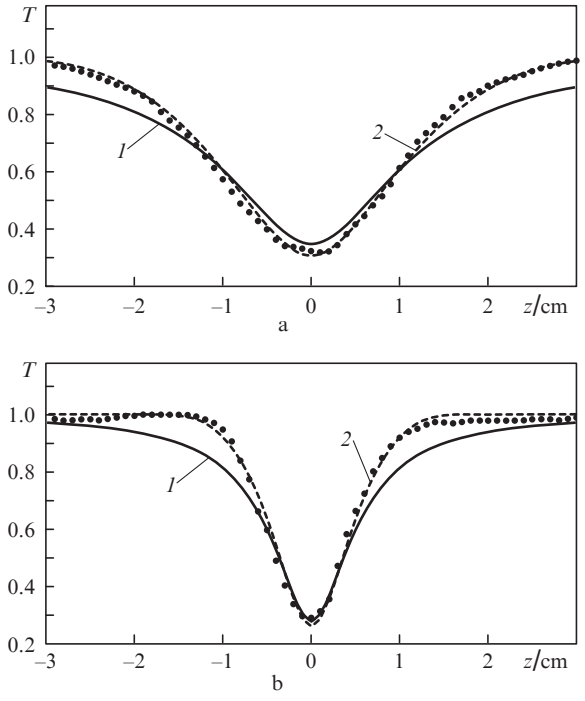

Figure 2. Experimental *z*-scan data (•) and theoretical curves calculated within the (*1*) non-threshold and (*2*) threshold models for (a) PEO/MWCNTs in DMF and (b) MWCNTs in DMF at an initial energy of 124 μJ.

In addition, we used (as in [33]) *z*-scan data from the published studies on the following media: zinc selenide ZnSe [6], porphyrin-graphene (Graphene-TPP) and fullerene-graphene (Graphene C_{60}) [28], and PEO/MWCNTs in DMF [16]. In all cases *z* scanning was performed using laser radiation with wavelength λ = 532 nm. At the same time, the initial pulse energy, pulse duration and thickness of working-medium layer in the limiter differed from experiment to experiment (Table 1). A specific feature of *z* scanning for the working media based on graphenes consisted in the use of several different initial pulse energies.

The results are listed in Table 1. Figure 2 shows examples of experimental *z*-scan curves in comparison with theoretical curves calculated within both threshold and non-threshold models. Figure 3 presents the output characteristics of limiters with the same working media as in Fig. 2.

4. Discussion

Based on the *z*-scan data for all working media, we calculated the values of nonlinear absorption coefficient β_c and threshold intensity I_c within the threshold model. For comparison, we also calculated the nonlinear absorption coefficient β within the non-threshold model (Table 1).

All the media under study can be divided into three groups. The media of the first group have a zero threshold intensity: $I_c = 0$. In this case, the data obtained within the threshold model coincide with the predictions of the non-

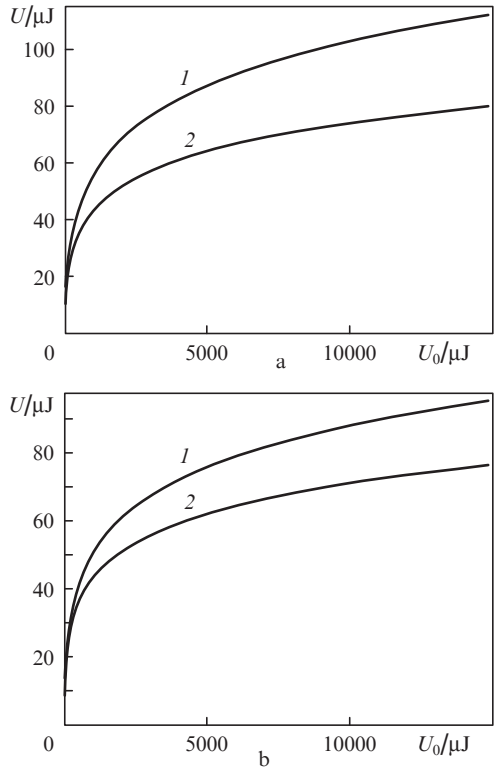

Figure 3. Output characteristics of limiters calculated within the (*1*) non-threshold and (*2*) threshold models for (a) PEO/MWCNTs in DMF and (b) MWCNTs in DMF at an initial energy of 124 μJ.

threshold model (the values of nonlinear absorption coefficients β and β_c are identical). This group contains working media based on MWCNTs in PMMA, SWCNTs in PMMA, DCM-684 in PGC, ZnSe, and Graphene-TPP (investigated at a laser wavelength of 532 nm) and MWCNTs in PMMA (studied at a wavelength of 1064 nm). One can assume that the threshold effect is absent for the first-group media.

The media of the second group are characterised by a low threshold intensity I_c. For these materials, the nonlinear absorption coefficients β and β_c differ only slightly. This group contains working media based on Graphene-C_{60}; MWCNTs in THF; and all dyes, except for DCM-684 in PGC; they were investigated at a laser wavelength of 532 nm. One can state that the threshold effect in the second-group media is weakly pronounced (if exists at all).

The advantages of the threshold model are most pronounced in the case of the third-group media, for which the threshold intensity I_c differs significantly from zero. The values of nonlinear absorption coefficients β and β_c also differ. This group includes working media based on MWCNTs and SWCNTs in DMF, SWCNTs in THF, and PEO/MWCNTs in DMF, which were investigated at a laser wavelength of 532 nm, and SWCNTs in PMMA and MWCNTs in DMF (studied at a wavelength of 1064 nm). Thus, the existence of threshold nonlinear interaction of laser radiation with the limiter working medium was experimentally proven for the third-group samples.

Using the found parameters of the media under study, one can calculate theoretical *z*-scan curves for the threshold and non-threshold models and compare them with experimental data. Figure 2 shows experimental *z*-scan data and theoretical curves calculated within the non-threshold and threshold models for PEO/MWCNTs in DMF and MWCNTs in DMF for a laser pulse with an initial energy of 124 μJ. It can clearly be seen that the predictions of the threshold model are in much better agreement with the experimental data.

For graphene-based working media, *z*-scan data were obtained at different initial pulse energies [28]. The nonlinear absorption coefficient was found to depend on the initial pulse energy (Table 1). Apparently, this may be caused by insufficient adequacy of the linear model (2) or (3) to the physical processes of interaction of high-power laser beam with the limiter working medium. In other words, the dependence of the absorption coefficient on the laser radiation intensity has a much more complex character or there is some physical process (in particular, radiation scattering [28]) disregarded by these models.

Knowing the parameters of the limiter working medium, i.e., α and β (for the non-threshold model), or α, β_c and I_c (for the threshold model), allows one to calculate the output characteristic for any other thicknesses of the limiter working medium and other values of initial radiation parameters, using expression (9) for the non-threshold model and (11)–(13) for the threshold model. The thus found parameters of the limiter working media (Table 1) were used to calculate the output characteristics of limiters for all media under consideration. The calculation was performed on the assumption that the laser beam is always focused on the working medium to obtain a maximum intensity and, therefore, to maximally attenuate radiation, whereas the input pulse energy was varied.

As one would expect, the output characteristics calculated within the threshold and non-threshold models coincide for the first-group working media.

For the second-group media, characterised by a low threshold intensity I_c, the output characteristics calculated within the threshold and non-threshold models differ only slightly.

The output characteristics of the third-group working media demonstrate a significant difference between the predictions of the threshold and non-threshold models. For example, Fig. 3 shows the output characteristics calculated within the non-threshold and threshold models for PEO/MWCNTs in DMF and MWCNTs in DMF and a laser pulse with an initial energy of 124 μJ. It can be seen that the non-threshold model underestimates the ability of these working media to limit the high-power laser intensity.

5. Conclusions

The threshold model proposed to describe the properties of high-power laser beam limiters takes into account the threshold character of nonlinear interaction between the laser radiation and limiter working medium. The generally accepted non-threshold model is a particular case of the threshold model if the threshold intensity is zero.

The threshold model, as well as the non-threshold one, allows one to use *z*-scan data to find the dependence of the absorption coefficient of a material under study on the radiation intensity and calculate the output characteristics of the limiter for different values of the working medium thickness and laser radiation parameters.

Based on experimental *z*-scan data, we determined the values of the nonlinear absorption coefficient and threshold intensity for the media under study (see table).

A threshold effect of nonlinear interaction of laser radiation with some working media based on SWCNTs and

MWCNTs was experimentally found. At the same time, the absence of this effect was proven for a number of materials.

It was shown that the predictions of the threshold model are much more consistent with experimental *z*-scan data.

Examples of output characteristics of laser radiation limiters, describing their nonlinear properties on the whole, were presented. It was shown that the non-threshold model may significantly underestimate the ability of a given working medium to limit the high-power laser radiation intensity.

Acknowledgements. This work was supported by the Ministry of Education and Science of the Russian Federation (State Contract No. 14.430.11.0006).

References

1. Guiliano C.R., Hess L.D. *IEEE J. Quantum Electron.*, **3**, 358 (1967).
2. Tutt L.W., Boggess T.F. *Prog. Quantum Electron.*, **17**, 299 (1993).
3. Ganeev R.A., Usmanov T.B. *Kvantovaya Elektron.*, **37** (7), 605 (2007) [*Quantum Electron.*, **37** (7), 605 (2007)].
4. Wang J., Blau W.J. *J. Opt. A: Pure Appl. Opt.*, **11**, 024001-1 (2009).
5. Zhi Bo Liu, Xiao Liang Zhang, Xiao Qing Yan, Yong Sheng Chen, Jian Guo Tian. *Chin. Sci. Bull.*, **57**, 2971 (2012).
6. Sheik-Bahae M., Said A.A., Wei T.H., Hagan D.J., Van Stryland E.W. *IEEE J. Quantum Electron.*, **26**, 760 (1990).
7. Kopylova T.N., Lugovskii A.P., Podgaetskii V.M., Ponomareva O.V., Svetlichnyi V.A. *Kvantovaya Elektron.*, **36** (3), 274 (2006) [*Quantum Electron.*, **36** (3), 274 (2006)].
8. Hsu J., Fuentes-Hernandez C., Ernst A.R., Hales J.M., Perry J.W., Kippelen B. *Opt. Express*, **20**, 8629 (2012).
9. Borissevitch I.E., Rakov N., Maciel G.S., Araujo C.B. *Appl. Opt.*, **39**, 4431 (2000).
10. Bala Murali Krishna M., Kumar V.P., Venkatramaiah N., Venkatesan R., Rao D.N. *Appl. Phys. Lett.*, **98**, 081106 (2011).
11. Wang A., Fang Y., Yu W., Long L., Song Y., Zhao W., Cifuentes M.P., Humphrey M.G., Zhang C. *Chem. Asian J.*, **9**, 639 (2014).
12. Gerasimenko A.Yu., Podgaetskii V.M. *Kvantovaya Elektron.*, **42** (7), 591 (2012) [*Quantum Electron.*, **42** (7), 591 (2012)].
13. Yellampalli S. *Carbon Nanotubes – Synthesis, Characterization, Applications* (Rijeka, Croatia: InTech, 2011) p. 514.
14. Muller O., Dengler S., Ritt G., Eberle B. *Appl. Opt.*, **52**, 139 (2013).
15. Hayden O., Nielsch K. *Molecular- and Nano-Tubes* (New York: Springer, 2011) p. 473.
16. Jin Z., Sun X., Xu G., Goh S.H., Ji W. *Chem. Phys. Lett.*, **318**, 505 (2000).
17. Belousova I.M., Danilov O.B., Videnichev D.A., Volynkin V.M., Vedenyapina Zh.B., Kislyakov I.M., Muranova G.A., Murav'eva T.D., Ryzhov A.A. *Opt. Zh.*, **80**, 18 (2013).
18. Wang A., Fang Y., Long L., Song Y., Yu W., Zhao W., Cifuentes M.P., Humphrey M.G., Zhang C. *Chem. Europ. J.*, **19**, 14159 (2013).
19. Liu Z., Guo Z., Zhang X., Zheng J., Tian J. *Carbon*, **51**, 419 (2013).
20. Gupta J., Vijayan C., Maurya S.K., Goswami D. *Opt. Commun.*, **285**, 1920 (2012).
21. Wang J., Liao K., Fruchtl D., Tian Y., Gilchrist A., Alley N.J., Andreoli E., Aitchison B., Nasibulin A.G., Byrne H.J., Kauppinen E.I., Zhang L., Blau W.J., Curran S.A. *Mater. Chem. Phys.*, **133**, 992 (2012).
22. Anand B., Podila R., Ayala P., Oliveira L., Philip R., Sai S.S., Zakhidovf A.A., Rao A.M. *Nanoscale*, **16**, 7271 (2013).
23. Zhang L., Wang L. *Polymer-plastics Technology Engineering*, **51**, 6 (2012).
24. Liaros N., Iliopoulos K., Stylianakis M.M., Koudoumas E., Couris S. *Opt. Mater.*, **36**, 112 (2013).
25. Kavitha M.K., Honey J., Pramod G., Reji P. *Mater. Chem. C*, **23**, 3669 (2013).
26. Zhang M., Li G., Li L. *Mater. Chem. C*, **8**, 1482 (2014).
27. Sun Z., Dong N., Xie K., Xia W., Konig D., Nagaiah T.C., Sanchez M.D., Ebbinghaus P., Erbe A., Zhang X., Ludwig A., Schuhmann W., Wang J., Muhler M. *Phys. Chem. C*, **117**, 11811 (2013).
28. Liu Z.B., Xu Y.F., Zhang X.Y., Zhang X.L., Chen Y.S., Tian J.G. *Phys. Chem. B*, **113**, 9681 (2009).
29. Cheng X., Dong N., Li B., Zhang X., Zhang S., Jiao J., Blau W.J., Zhang L., Wang J. *Opt. Express*, **21**, 16486 (2013).
30. Ouyang Q., Xu Z., Lei Z., Dong H., Yu H., Qi L., Li C., Chen Y. *Carbon*, **67**, 214 (2014).
31. Xiaoqing Z., Miao F., Zhan H. *Mater. Chem. C*, **41**, 6759 (2013).
32. Lim G., Chen Z., Clark J., Goh R.G.S., Ng W., Tan H., Friend R.H., Ho P.K.H., Chua L. *Nat. Photonics*, **5**, 554 (2011).
33. Tereshchenko S.A., Podgaetskii V.M., Gerasimenko A.Yu., Savel'ev M.S. *Opt. Spektrosk.*, **116**, 486 (2014).
34. Tereshchenko S.A., Podgaetskii V.M. *Kvantovaya Elektron.*, **41** (1), 26 (2011) [*Quantum Electron.*, **41** (1), 26 (2011)].
35. Belousova I.M., Danilov O.B., Sidorov A.I. *Opt. Zh.*, **76**, 71 (2009).